# Doubly excited $^{1,3}P^e$ resonance states of helium and the hydrogen negative ion interacting with Coulomb and screened Coulomb potentials

Sabyasachi Kar[1,*] and Y. K. Ho[2,†]

[1]*Center for Theoretical Atomic and Molecular Physics, The Academy of Fundamental and Interdisciplinary Sciences, Harbin Institute of Technology, Harbin 150080, People's Republic of China*
[2]*Institute of Atomic and Molecular Sciences, Academia Sinica, P.O. Box 23-166, Taipei, Taiwan 106, Republic of China*

We have investigated the doubly excited $^{1,3}P^e$ resonance states of helium and the hydrogen negative ion interacting with Coulomb and screened Coulomb potentials using exponential correlated wave functions. In the pure Coulomb case, calculations have been carried out by using the complex-coordinate rotation and the stabilization method. The $^1P^e$ resonance states of He below the $N = 3$, 4, and 5 thresholds of He$^+$, and the $^3P^e$ resonance states of He below the $N = 3$ thresholds of He$^+$, are reported. The $5p^2\ ^3P^e$ state, which has attracted recent interest, is also reported and discussed. In the screened Coulomb case, we have used the stabilization method to obtain two different series ($3pnp$ and $3dnd$) of resonance states below the $N = 3$ He$^+$ threshold as a function of the screening parameters. Resonance widths for the $3dnd$ series show some interesting behaviors. The resonance parameters (position and width) for helium and the hydrogen negation ion as functions of the screening parameters are reported.

PACS number(s): 31.15.vj, 34.80.Bm, 31.15.xt, 52.20.Fs

## I. INTRODUCTION

Studies of the structural properties of helium and the hydrogen negative ion interacting with screened Coulomb potentials are of great interest in recent years [1–16]. Investigations on the doubly excited resonance states of two-electron systems are of special interest to predict the behavior of resonance states for increasing screening strength [2,4–6,8,9,16–18]. In the past several years, we have initiated resonance calculations for different atomic and molecular systems [2,9,18]. We have also studied the doubly excited $^{1,3}P^e$ resonance states of He interacting with screened Coulomb interactions using configuration interaction (CI)–type wave functions with some approximation in the atomic Hamiltonian [19]. In the present work, our main interest is to report the behavior of the $^{1,3}P^e$ resonance parameters of helium in the stronger screening region and the $^{1,3}P^e$ resonance states of the hydrogen negative ion interacting with screened Coulomb potentials using correlated wave functions.

In the pure Coulomb case, here we have investigated the $^1P^e$ resonance states of He below the $N = 3$, 4, and 5 thresholds of He$^+$. Recently we have reported the $^3P^e$ resonance states of helium below the $N = 4$ and 5 He$^+$ threshold [20]. It is well known that for a doubly excited resonance associated with and below a high-threshold $N$ of the one-electron parent system, such a resonance may lie below the $(N - 1)$th threshold if $N$ is sufficiently high and/or if Z is sufficiently large. Due to a recent report [21], we have also presented the $5p^2\ ^3P^e$ resonance states of the helium atom in detail. Studies on the $^{1,3}P^e$ resonance states of He [22–26] and H$^-$ [27–31] have also been reported in the literature. Several experiments have been performed on the doubly excited $^3P^e$ state [32,33]. Our results are comparable with the reported results, and few $^1P^e$ resonance states are reported using correlated wave functions.

To extract resonance parameters, we have used the stabilization method [34–36] and the complex-coordinate rotation method [37]. We employ correlated exponential basis functions to represent the correlation effect between the charged particles.

In the screened Coulomb case, we have investigated the $^{1,3}P^e$ resonance states of helium and H$^-$ below the $N = 3$ threshold using highly correlated wave functions in the framework of the stabilization method. In the case of the screened helium atom, we compare our present results using correlated basis functions with those reported by us using CI-type basis functions [19]. In the present work, using correlated basis functions, we have obtained two series of resonance states of He, of which the $3dnd$ series shows some interesting behaviors in between the $3S$ and $3P$ thresholds of the He$^+$ ion. Such behaviors have not been observed in our previous work [19] using CI-type basis functions. In the case of the hydrogen negative ion, no other calculations are reported for $^{1,3}P^e$ states with screened Coulomb interactions. The atomic unit has been used throughout the work.

## II. HAMILTONIAN AND WAVE FUNCTIONS

The nonrelativistic Hamiltonian describing the helium atom and the hydrogen negative ion in the screening environments is given by

$$H = T + V = -\frac{1}{2}\nabla_1^2 - \frac{1}{2}\nabla_2^2$$
$$- Z\left[\frac{\exp(-\mu r_1)}{r_1} + \frac{\exp(-\mu r_2)}{r_2}\right] + \frac{\exp(-\mu r_{12})}{r_{12}}, \quad (1)$$

where $r_1$ and $r_2$ are the radial coordinates of the two electrons and $r_{12}$ is their relative distance. When the helium atom is placed in a vacuum, we have $\mu = 0$. In plasma physics, the parameter $\mu$ (where $\mu = 1/D$, D is called Debye length) is known as the Debye screening parameter.

*skar@hit.edu.cn
†ykho@pub.iams.sinica.edu.tw

TABLE I. Doubly excited $^1P^e$ resonance states of He below the $N=3$ He$^+$ threshold, $E_{th}(N=3) = -0.22222222$. The numbers in the square brackets denote the powers of ten. The numbers in the parentheses show the uncertainty in the last digit.

| States | Present work[a] | | | | Other calculations using Complex-rotation method | |
|---|---|---|---|---|---|---|
| | Complex-rotation method | | Stabilization method | | | |
| | $E_r$ | $\Gamma/2$ | $E_r$ | $\Gamma/2$ | $E_r$ | $\Gamma/2$ |
| 3p4p | −0.27899253 | 0.22152[−4] | −0.27899202 | 0.222[−4] | −0.2789925[b] | 0.223[−4][b] |
| 3d4d | −0.25935204 | 0.630[−6] | −0.25935203 | 0.632[−6] | −0.259352[b] | 0.6295[−6][b] |
| 3p5p | −0.25363872 | 0.131977[−4] | −0.2536384 | 0.132[−4] | −0.2536387[b] | 0.131925[−4][b] |
| 3d5d | −0.24451362 | 0.435[−6] | −0.2445136 | 0.434[−6] | −0.2445136[b] | 0.4375[−6][b] |
| 3p5p | −0.2422375 | 0.769[−5] | −0.2422373 | 0.77[−5] | −0.242237[b] | 0.8[−5][b] |
| 3d5d | −0.23728242 | 0.29[−6] | −0.2372824 | 0.32[−6] | −0.237282423[c] | 0.29[−6][c] |
| 3p6p | −0.2360989 | 0.47[−5] | −0.2360984 | 0.48[−5] | −0.23609888[c] | 0.475[−5][c] |
| 3d6d | −0.2331134 | 0.2(1)[−6] | −0.233113 | 0.2(2)[−6] | −0.231144072[c] | 0.1971[−6][c] |
| 3p7p | −0.232411 | 0.3[−5] | −0.232410 | 0.3[−5] | −0.232410753[c] | 0.3104[−5][b] |

[a]Using exponential wave functions.
[b]Ho and Bhatia, using Hylleraas-type wave functions [23].
[c]Eiglsperger, Piraux, and Madronero, using Coulomb-Strumian basis functions [26].

TABLE II. Doubly excited $^1P^e$ resonance states of helium below the $N=4$ and $N=5$ He$^+$ thresholds using complex-coordinate rotation method, along with effective quantum numbers $n^*$ and effective resonance widths $(n^*)^3\,\Gamma$. The numbers in the square brackets denote the powers of ten. The numbers in the parentheses show the uncertainty in the last digit.

| States | Present work[a] | | Other calculations | | Present work | |
|---|---|---|---|---|---|---|
| | $E_r$ | $\Gamma/2$ | $E_r$ | $\Gamma/2$ | $n^*$ | $(n^*)^3\,\Gamma$ |
| $E_{th}(N=4) = -0.125$ | | | | | | |
| 4p5p | −0.16551929 | 0.3481[−4] | −0.1655193[b] | 0.348[−4][b] | 3.5128054 | 0.00301784 |
| 4d5d | −0.15640849 | 0.4202[−4] | −0.1564085[b] | 0.420[−4][b] | 3.9898951 | 0.00536077 |
| 4p6p | −0.1496610 | 0.264[−4] | −0.149660985[b] | 0.264[−4][b] | 4.5027689 | 0.00482029 |
| 4d6d | −0.1452223 | 0.56[−5] | −0.14522225[b] | 0.56[−5][b] | 4.9724420 | 0.00137698 |
| 4f5f | −0.1442326 | 0.2288[−3] | −0.1442325[b] | 0.22885[−3][b] | 5.0987768 | 0.00233320 |
| 4p7p | −0.1415795 | 0.176[−4] | −0.141578[b] | 0.175[−4][b] | 5.4916049 | 0.00582962 |
| 4d7d | −0.1387785 | 0.46[−5] | −0.138778490[c] | 0.4604[−5][c] | 6.0239871 | 0.00201113 |
| 4f6f | −0.1382318 | 0.14[−4] | −0.13823181[c] | 0.1404[−4][c] | 6.1471745 | 0.00650406 |
| 4p8p | −0.136894 | 0.12[−4] | −0.136894328[c] | 0.11765[−4][c] | 6.4836720 | 0.00654145 |
| 4d8d | −0.1350694 | 0.3[−5] | −0.1350694494[c] | 0.32298[−5][c] | 7.0466582 | 0.00209943 |
| 4f7f | −0.13472 | 0.9(1)[−5] | −0.134717582[c] | 0.9398[−5][c] | 7.1721914 | 0.00664092 |
| 4p9p | −0.13394 | 0.2(1)[−4] | −0.133941318[c] | 0.8109[−5][c] | 7.4785300 | 0.01673049 |
| $E_{th}(N=5) = -0.08$ | | | | | | |
| 5p6p | −0.1099271 | 0.36[−4] | −0.10992705[b] | 0.3633[−4][b] | 4.0874522 | 0.00491689 |
| 5d6d | −0.105180 | 0.64(1)[−4] | −0.10517915[b] | 0.641[−4][b] | 4.4561227 | 0.01132613 |
| 5p6f | −0.099588 | 0.32(1)[−4] | −0.099588[b] | 0.32[−4][b] | 5.0523096 | 0.00825372 |
| 5p7p | −0.099133 | 0.42[−4] | −0.0991315[b] | 0.405[−4][b] | 5.1120309 | 0.01122173 |
| 5d7d | −0.09635 | 0.55[−4] | −0.096355[b] | 0.5[−4][b] | 5.5300126 | 0.01860249 |
| 5f7f | −0.093797 | 0.24[−4] | −0.09379757[c] | 0.2374[−4][c] | 6.0199470 | 0.01047175 |
| 5p8p | −0.092842 | 0.3[−4] | −0.09284200[c] | 0.2789[−4][c] | 6.2397713 | 0.01457663 |
| 5g6g | −0.092086 | 0.2[−5] | −0.092085843[c] | 0.1652[−4][c] | 6.4319655 | 0.00106437 |
| 5d8d | −0.09160 | 0.4[−4] | −0.09159661[c] | 0.3609[−4][c] | 6.5653216 | 0.02263904 |
| 5f8f | −0.09022 | 0.2[−4] | −0.09021782[c] | 0.1700[−4][c] | 6.9945464 | 0.01368796 |
| 5p9p | −0.08940 | 0.2[−4] | −0.08939833[c] | 0.1844[−4][c] | 7.2932496 | 0.01551755 |
| 5g7g | −0.08899 | 0.5[−5] | −0.088983560[c] | 0.2856[−5][c] | 7.4577042 | 0.00414778 |
| 5d9d | −0.0886 | 0.4(1)[−4] | −0.08868311[c] | 0.2552[−4][c] | 7.6249285 | 0.03546478 |
| 5f9f | −0.0879 | 0.2[−4] | −0.087857284[c] | 0.12278[−4][c] | 7.9555728 | 0.02014069 |

[a]Using exponential wave functions.
[b]Ho and Bhatia, using Hylleraas-type wave functions [23].
[c]Eiglsperger, Piraux, and Madronero, using Coulomb-Strumian basis functions [26].

For singlet- and triplet-$P$ unnatural parity states of the He atom, we employ highly correlated wave functions [1,2,9,31,39,40],

$$\Psi = (1 + S_{pn}\hat{P}_{12}) \sum_{i=1}^{N_b} \sum_{l_1=\varepsilon}^{L} A_i(-1)^\varepsilon Y_{LM}^{l_1,l_2}(\mathbf{r}_1,\mathbf{r}_2)$$

$$\times \exp\left[(-\alpha_i r_1 - \beta_i r_2 - \gamma_i r_{12})\omega\right], \quad (2)$$

with

$$Y_{LM}^{l_1,l_2}(\mathbf{r}_1,\mathbf{r}_2) = r_1^{l_1} r_2^{l_2} \sum_{m_1,m_2} C_{l_1 m_1, l_2 m_2}^{LM} Y_{l_1 m_1}(\hat{r}_1) Y_{l_2 m_2}(\hat{r}_2), \quad (3)$$

where the functions $Y_{LM}^{l_1,l_2}(\mathbf{r}_1,\mathbf{r}_2)$ are the bipolar harmonics or Schwartz harmonics, $\hat{r}_i = \mathbf{r}_i/r_i$ $(i = 1, 2)$, $Y_{l_i m_i}(\hat{r}_i)$ denotes the usual spherical harmonics, $C_{l_1 m_1, l_2 m_2}^{LM}$ are the Clebsch-Gordan coefficients, $\alpha_i, \beta_i, \gamma_i$ are the nonlinear variation parameters, $A_i (i = 1, ..., N)$ are the linear expansion coefficients, $l_1 + l_2 = L + \varepsilon$, $L = 1$, $\varepsilon = 1$, $N_b$ is the number of basis terms, and the operator $\hat{P}_{12}$ is the permutation of the two identical particles 1 and 2. $S_{pn}$ denotes the spin functions. The scaling factor $\omega$ is set equal to 1 for bound-states calculations and is varied for resonance-states calculations. The nonlinear variational parameters $\alpha_i, \beta_i$, and $\gamma_i$ are chosen from a quasirandom process [1,2,9,18,31,39,40]. The exponential wave functions supported by the quasirandom process are widely used in several other works [4,5,27–29].

## III. RESULTS WITH COULOMB INTERACTIONS

We have used the complex-coordinate rotation method and the stabilization method to extract resonance parameters in the pure Coulomb interaction. In the complex-coordinate rotation method [17,38,40], the interparticle radial coordinate $r_{ij}$ is transformed into $r_{ij} = r_{ij} \exp(i\theta)$, where $\theta$ is real and positive. The Hamiltonian $H$ takes the form

$$H = T \exp(-2i\theta) + V \exp(-i\theta). \quad (4)$$

Resonance position can be identified by observing the complex energy levels $E(\theta, \omega)$, and a complex resonance eigenvalue $W = E_r - i\Gamma/2$, where $E_r$ and $\Gamma$ denote the resonance energy and width, respectively. Details of the complex-coordinate rotation are available from the previous review article [38]. In the stabilization method, the resonance can be identified from the flat plateau of the stabilization diagram drawn by plotting the energy levels $E(\omega)$ versus $\omega$. We then calculate the density of the resonance states in the stabilized parts of the energy levels, with one stabilized plateau at a time, using the formula used in our previous works [2,9,18,19,36]. The density of states of each plateau energy level is then fitted to the Lorentzian form [2,9,18,19,36] to extract resonance parameters ($E_r$, $\Gamma$) for a particular set of resonance states. From the best fit with the least chi-square, and the square of the correlation coefficient close to 1, it will give the desired resonance energy $E_r$ and width $\Gamma$. For the detailed computational aspect of the stabilization method, readers are referred to earlier works of Ho and coworkers [2,9,18,19,36,40]. We have presented $^1P^e$ resonance parameters ($E_r$, $\Gamma$) obtained using the complex-coordinate rotation method below the $N = 3$, 4, and 5 thresholds of the He$^+$ ion in Tables I and II. The resonance energies and widths for the $^3P^e$ states lying below the $N = 3$ He$^+$ threshold are presented in Table III. We have presented the $^3P^e$ resonance states of He below the $N = 4$ and 5 thresholds in our previous works [20]. Results for resonances lying below the $N = 3$ threshold obtained from the stabilization method are presented in Tables I and III. Our results for the He atom are comparable

TABLE III. Doubly excited $^3P^e$ resonance states of He below the $N = 3$ He$^+$ threshold, $E_{th}$ $(N = 3) = -0.22222222$ a.u. The numbers in the square brackets denote the powers of ten. The numbers in the parentheses show the uncertainty in the last digit.

| | Present work[a] | | | | Other work using | | Other calculations using | |
| | Complex-rotation method | | Stabilization method | | Stabilization method[b] | | Complex-rotation method | |
| States | $E_r$ | $\Gamma/2$ | $E_r$ | $\Gamma/2$ | $E_r$ | $\Gamma/2$ | $E_r$ | $\Gamma/2$ |
|---|---|---|---|---|---|---|---|---|
| $3p3p$ | −0.33608791 | 0.2244376[−2] | −0.33610 | 0.223[−2] | −0.33607 | 0.227[−2] | −0.3360879[c] | 0.224435[−2][c] |
| $3d3d$ | −0.291158224 | 0.37002[−4] | −0.291158 | 0.372[−4] | −0.29116 | 0.350[−4] | −0.291158225[c] | 0.370[−4][c] |
| $3p4p$ | −0.27155715 | 0.89432[−3] | −0.27154 | 0.895[−3] | −0.27156 | 0.885[−3] | −0.27155715[c] | 0.89435[−3][c] |
| $3d4d$ | −0.253574652 | 0.117616[−4] | −0.253574 | 0.118[−4] | −0.25357 | 0.100[−4] | −0.25357465[c] | 0.117615[−4][c] |
| $3p5p$ | −0.2509316 | 0.42766[−3] | −0.25093 | 0.427[−3] | −0.25093 | 0.425[−3] | −0.2509315[c] | 0.4275[−3][c] |
| $3d5d$ | −0.24195829 | 0.722[−5] | −0.241958 | 0.724[−5] | −0.24196 | 0.500[−5] | −0.2419583[c] | 0.72[−5][c] |
| $3p6p$ | −0.240960 | 0.228[−3] | −0.24096 | 0.225[−3] | −0.24096 | 0.225[−3] | −0.24096[c] | 0.225[−3][c] |
| $3d6d$ | −0.2358942 | 0.47[−5] | −0.235894 | 0.475[−5] | −0.23589 | 0.467[−5] | −0.2358935[c] | 0.40[−5][c] |
| $3p7p$ | −0.235396 | 0.133[−3] | −0.235395 | 0.131[−3] | −0.23539 | 0.135[−3] | −0.2353963[d] | 0.1336[−3][d] |
| $3d7d$ | −0.232271 | 0.3[−5] | −0.23227 | 0.367[−5] | −0.23227 | 0.316[−5] | −0.23227095[d] | 0.318[−5][d] |
| $3p8p$ | −0.23198 | 0.8(1)[−4] | −0.23198 | 0.85[−4] | −0.23198 | 0.85[−4] | −0.2319828[d] | 0.846[−4][d] |
| $3d8d$ | −0.22992 | 0.2(1)[−5] | | | −0.22992 | 0.2245[−5] | −0.22992382[d] | 0.225[−5][d] |
| $3p9p$ | −0.2297 | 0.58(1)[−4] | | | −0.22974 | 0.55[−4] | −0.2297407[d] | 0.568[−4][d] |

[a]Using exponential wave functions.
[b]Saha and Mukherjee, using Hylleraas-type wave functions [25].
[c]Ho and Bhatia, using Hylleraas-type wave functions [23].
[d]Eiglsperger, Piraux, and Madronero, using Coulomb-Strumian basis functions [26].

TABLE IV. Doubly excited $3p4p$ $^{1,3}P^e$ states of H$^-$ for different values of the screening parameter $D$, along with the H($3p$ $^2P$) threshold energy.

| $D$ | $3p4p$ $^1P^e$ | | $3p4p$ $^3P^e$ | | |
|---|---|---|---|---|---|
| | $E_r$ | $\Gamma(10^{-5})$ | $E_r$ | $\Gamma(10^{-4})$ | H($3p^2P$) |
| $\infty$ | $-0.056402199$ | $0.380$ | $-0.05591058$ | $0.8394$ | $-0.055555555$ |
| 200 | $-0.051486477$ | $0.374$ | $-0.05100327$ | $0.8220$ | $-0.050708224$ |
| 100 | $-0.046766790$ | $0.351$ | $-0.04631752$ | $0.7264$ | $-0.046153105$ |
| 80 | $-0.044490514$ | $0.333$ | $-0.04407105$ | $0.6383$ | $-0.043979583$ |
| 70 | $-0.042901121$ | $0.316$ | $-0.04250773$ | $0.57$ | $-0.042468034$ |
| 60 | $-0.040831315$ | $0.290$ | $-0.04049089$ | $0.37$ | $-0.040504461$ |
| 50 | $-0.038033076$ | $0.243$ | | | $-0.037852389$ |
| 45 | $-0.036236137$ | $0.203$ | | | $-0.036145512$ |
| 41 | $-0.034541440$ | $0.148$ | | | $-0.034526265$ |
| 40 | $-0.034076932$ | $0.135$ | | | $-0.034078910$ |

with the available results in the literature [22–24,26]. The $^3P^e$ resonance below the $N = 3$ threshold is comparable with those reported by Saha *et al.* [25].

Here we present details of the $5p^2$ $^3P^e$ resonance state of helium, in context with the recent report [21]. The $5p^2$ $^3P^e$ state (approximate configuration) is an intruder state. Lying below the $N = 4$ manifold ($E_{th} = -0.125$ a.u.) an intruder state (also called perturber) is a state that belongs, due to its quantum numbers, to a Rydberg series of a higher manifold (in this case, $N = 5$ with threshold energy $E_{th} = -0.08$ a.u.) [24]. Figure 1 shows the rotational path for the $5p^2$ $^3P^e$ state of He for five different values of $\omega$. The $5p^2$ $^3P^e$ resonance parameters $\{E_r, \Gamma\}$ in atomic units are determined [20] as $\{-0.126378(2), 0.002174(1)\}$, which are comparable with
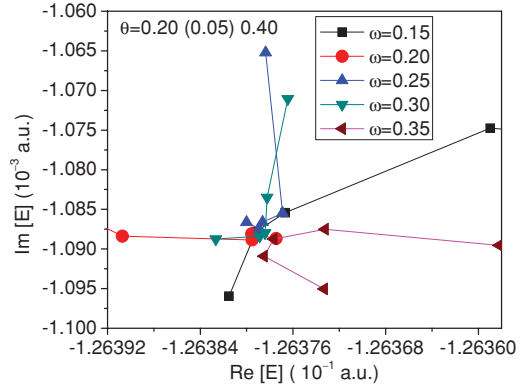


FIG. 1. (Color online) Rotational paths for the $5p^2$ $^3P^e$ resonance in the energy plane for 5 different values of the scaling factor $\omega$.

the results $\{-0.12608(2), 0.0024(6)\}$ reported by Argenti and Moccia [24] and $\{-0.12639, 0.00217\}$ reported by Ho and Bhatia [23].

To classify the resonance states below the $N = 4$ and $N = 5$ thresholds of the He$^+$ ion, we have calculated the effective widths $(n^*)^3\Gamma$. The effective quantum number $n^*$ for the $^{1,3}P^e$ resonance states are obtained using the formula

$$ E = -\frac{1}{2}\left[\left(\frac{Z}{N}\right)^2 + \left(\frac{Z-1}{n^*}\right)^2\right], \qquad (5) $$

where $N$, $E$, and $Z$ denote the inner-electron quantum number, the energy of the state below the total ionization, and the atomic number, respectively. We present the effective quantum numbers and the effective resonance widths in Table II. Our calculated resonance parameters are in good accord with the

TABLE V. Doubly excited $^1P^e$ resonance states of He for selected values of the screening parameters, along with the He$^+$($3s$ $^2S$) and He$^+$($3p$ $^2P$) thresholds.

| $D$ | $3p4p$ | | $3p5p$ | | $3d4d$ | | $3d5d$ | | H($3s$ $^2S$) | H($3p$ $^2P$) |
|---|---|---|---|---|---|---|---|---|---|---|
| | $E_r$ | $\Gamma(10^{-4})$ | $E_r$ | $\Gamma(10^{-4})$ | $E_r$ | $\Gamma(10^{-5})$ | $E_r$ | $\Gamma(10^{-5})$ | | |
| 100 | $-0.2501137$ | $0.436$ | $-0.2252359$ | $0.253$ | $-0.2307138$ | $0.134$ | $-0.2164788$ | $0.104$ | $-0.2028807139$ | $-0.2028328967$ |
| | $-0.2499845^a$ | $0.4345^a$ | $-0.225107^a$ | $0.256$ | $-0.2304445^a$ | $0.127^a$ | $-0.2162005^a$ | $0.0845^a$ | | |
| 50 | $-0.2233712$ | $0.410^a$ | $-0.1997510$ | $0.216$ | $-0.2046015$ | $0.156$ | $-0.1919006$ | $0.159$ | $-0.1847954312$ | $-0.1846124193$ |
| | $-0.222928^a$ | $0.413$ | $-0.199318^a$ | $0.218^a$ | $-0.2036151^a$ | $0.141^a$ | | | | |
| 25 | $-0.1757944$ | $0.329$ | $-0.1563713$ | $0.110$ | $-0.1591371$ | $0.299$ | $-0.151832$ | $0.31$ | $-0.1520800576$ | $-0.1514095568$ |
| 24 | $-0.1721670$ | $0.321$ | $-0.1531676$ | $0.098$ | $-0.1557348$ | $0.325$ | $-0.149050$ | $0.23$ | $-0.1495488353$ | $-0.1488266142$ |
| 23 | $-0.1682810$ | $0.313$ | $-0.1497503$ | $0.085$ | $-0.1521051$ | $0.356$ | $-0.146118$ | $0.15$ | $-0.1468300469$ | $-0.1460499126$ |
| 22 | $-0.1641089$ | $0.304$ | $-0.1460955$ | $0.071$ | $-0.1482288$ | $0.402$ | | | $-0.1439023716$ | $-0.1430571091$ |
| 21 | $-0.1596194$ | $0.294$ | $-0.1421753$ | $0.054$ | $-0.1440876$ | $0.451$ | | | $-0.1407412076$ | $-0.1398223619$ |
| 20 | $-0.1547766$ | $0.279$ | $-0.1379528$ | $0.035$ | $-0.1396672$ | $0.525$ | | | $-0.1373180396$ | $-0.1363156417$ |
| | $-0.152712^a$ | $0.282^a$ | | | | | | | | |
| 19 | $-0.1495397$ | $0.267$ | $-0.1333823$ | $0.017$ | $-0.1349621$ | $0.592$ | | | $-0.1335996649$ | $-0.1325018816$ |
| 18 | $-0.1438616$ | $0.250$ | | | $-0.1299757$ | $0.614$ | | | $-0.1295472422$ | $-0.1283399280$ |
| 17 | $-0.1376901$ | $0.238$ | | | $-0.1247071$ | $0.547$ | | | $-0.1251151265$ | $-0.1237812428$ |
| 16 | $-0.1309650$ | $0.217$ | | | $-0.1191338$ | $0.391$ | | | $-0.1202494429$ | $-0.1187683007$ |
| 15 | $-0.1236192$ | $0.194$ | | | $-0.1132334$ | $0.235$ | | | $-0.1148863620$ | $-0.1132326250$ |
| 14 | $-0.1155792$ | $0.169$ | | | | | | | $-0.1089500531$ | $-0.1070924201$ |
| 11 | $-0.0865573$ | $0.079$ | | | | | | | $-0.0867148894$ | $-0.0839683928$ |
| 10 | $-0.0751081$ | $0.044$ | | | | | | | $-0.0774102193$ | $-0.0742310075$ |

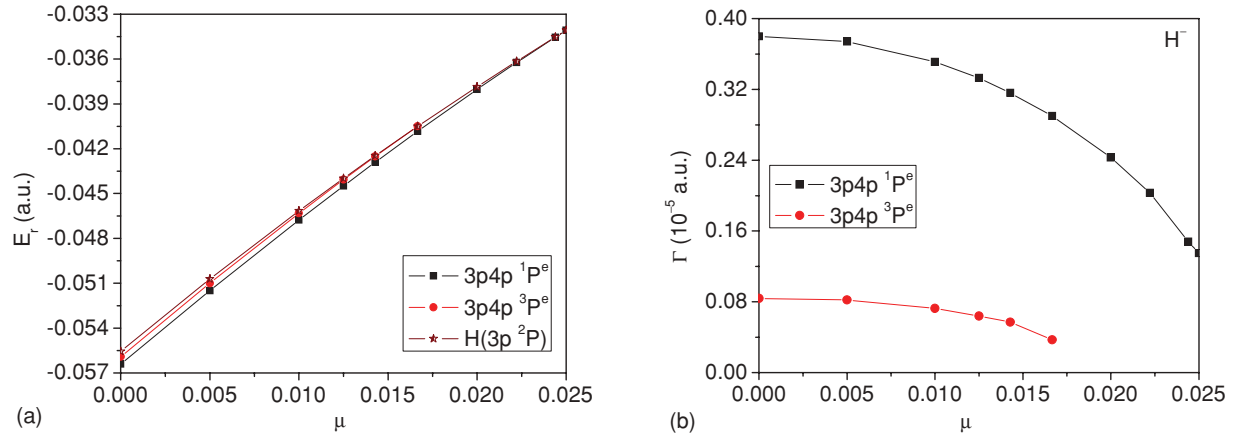[a]Our previous work with CI-type basis functions [19].

FIG. 2. (Color online) The $3p4p$ $^{1,3}P^e$ resonance (a) energies and (b) widths of H$^-$ in terms of the screening parameter $\mu$ (units of $a_0^{-1}$), along with the H($3p$ $^2P$) threshold energies.

reported results of Ho and Bhatia [2], and also in agreement with the recent work using the CI-type approach [26]. Ho and Bhatia have employed correlated Hylleraas-type wave functions involving the powers of interparticle distances. We have used the complex-coordinate rotation method [38] (dilatation transformation technique) in the present work. There are further developments beyond the original rotation technique to solve the resonance problem. These developments [41–46] are based on the complex virial theorem to determine stationarity and higher-order sum rules to determine the stability of the calculated solutions.

## A. RESULTS WITH SCREENED COULOMB INTERACTIONS

In our earlier work [19], we presented the $^{1,3}P^e$ resonance states of He using CI-type basis functions. In that study we made an approximation of the Hamiltonian. In the present work, we have investigated the effect of screening Coulomb potentials on He and H$^-$ using correlated exponential wave functions in the framework of the stabilization method. All of the results obtained from the present calculations are presented in Tables IV–VI and Figs. 2–6. As found in our previous investigation, resonance energies are decreasing

TABLE VI. Doubly excited $^3P^e$ resonance states of He for selected values of the screening parameters, along with the He$^+$($3s$ $^2S$) and He$^+$($3p$ $^2P$) thresholds.

| | 3p3p | | 3p4p | | 3d3d | | 3d4d | | | |
|---|---|---|---|---|---|---|---|---|---|---|
| $D$ | $E_r$ | $\Gamma$ ($10^{-2}$) | $E_r$ | $\Gamma$ ($10^{-2}$) | $E_r$ | $\Gamma$ ($10^{-4}$) | $E_r$ | $\Gamma$ ($10^{-4}$) | H($3s$ $^2S$) | H($3p$ $^2P$) |
| 100 | $-0.30692$ | 0.446 | $-0.24276$ | 0.1763 | $-0.262075$ | 0.763 | $-0.225103$ | 0.292 | $-0.2028807139$ | $-0.2028328967$ |
| | $-0.30671^a$ | $0.4515^a$ | $-0.242615^a$ | $0.1775^a$ | $-0.26185^a$ | $0.735^a$ | $-0.2248255^a$ | $0.265^a$ | | |
| 50 | $-0.27933$ | 0.440 | $-0.21628$ | 0.1657 | $-0.234750$ | 0.817 | $-0.199435$ | 0.503 | $-0.1847954312$ | $-0.1846124193$ |
| | $-0.27881^a$ | $0.4415^a$ | $-0.215785^a$ | $0.1695^a$ | $-0.23394^a$ | $0.77^a$ | $-0.19848^a$ | $0.4595^a$ | | |
| 20 | $-0.20549$ | 0.403 | $-0.14911$ | 0.1180 | $-0.162458$ | 1.230 | $-0.137739$ | 2.689 | $-0.1373180396$ | $-0.1363156417$ |
| | $-0.20328^a$ | $0.415^a$ | $-0.146915^a$ | $0.123^a$ | $-0.15840^a$ | $1.08^a$ | | | | |
| 19 | $-0.19962$ | 0.399 | $-0.14403$ | 0.1123 | $-0.156771$ | 1.290 | $-0.133430$ | 2.335 | $-0.1335996649$ | $-0.1325018816$ |
| 18 | $-0.19321$ | 0.394 | $-0.13854$ | 0.1058 | $-0.150571$ | 1.364 | $-0.128827$ | 1.885 | $-0.1295472422$ | $-0.1283399280$ |
| 17 | $-0.18619$ | 0.388 | $-0.13259$ | 0.0983 | $-0.143789$ | 1.457 | $-0.123920$ | 1.276 | $-0.1251151265$ | $-0.1237812428$ |
| 16 | $-0.17846$ | 0.381 | $-0.12612$ | 0.0893 | $-0.136346$ | 1.578 | $-0.118681$ | 0.727 | $-0.1202494429$ | $-0.1187683007$ |
| 15 | $-0.16991$ | 0.373 | $-0.11907$ | 0.0786 | $-0.128149$ | 1.743 | $-0.113034$ | 0.52 | $-0.1148863620$ | $-0.1132326250$ |
| 13 | $-0.14985$ | 0.351 | $-0.10296$ | 0.0493 | $-0.109060$ | 2.367 | | | $-0.1023503636$ | $-0.1002498194$ |
| 12 | $-0.13800$ | 0.336 | $-0.09375$ | 0.0275 | $-0.097970$ | 3.090 | | | $-0.0949804354$ | $-0.0925879412$ |
| 11 | $-0.12463$ | 0.319 | | | $-0.085972$ | 4.47 | | | $-0.0867148894$ | $-0.0839683928$ |
| 10.8 | $-0.12180$ | 0.313 | | | $-0.083546$ | 4.50 | | | $-0.0849419562$ | $-0.0821158159$ |
| 10.5 | $-0.11736$ | 0.307 | | | $-0.07996$ | 4.20 | | | $-0.0822020129$ | $-0.0792501924$ |
| 10 | $-0.10960$ | 0.294 | | | $-0.07419$ | 2.58 | | | $-0.0774102193$ | $-0.0742310075$ |
| | $-0.10266^a$ | $0.320^a$ | | | | | | | | |
| 9.7 | $-0.10470$ | 0.286 | | | $-0.07079$ | 1.80 | | | $-0.0743930606$ | $-0.0710657194$ |
| 9.5 | $-0.10134$ | 0.281 | | | $-0.06852$ | 1.58 | | | $-0.072319807$ | $-0.0688884703$ |
| 7 | $-0.05184$ | 0.178 | | | | | | | $-0.0418424192$ | $-0.0366985077$ |
| 5 | $-0.00702$ | 0.031 | | | | | | | $-0.0128321869$ | $-0.0063560019$ |

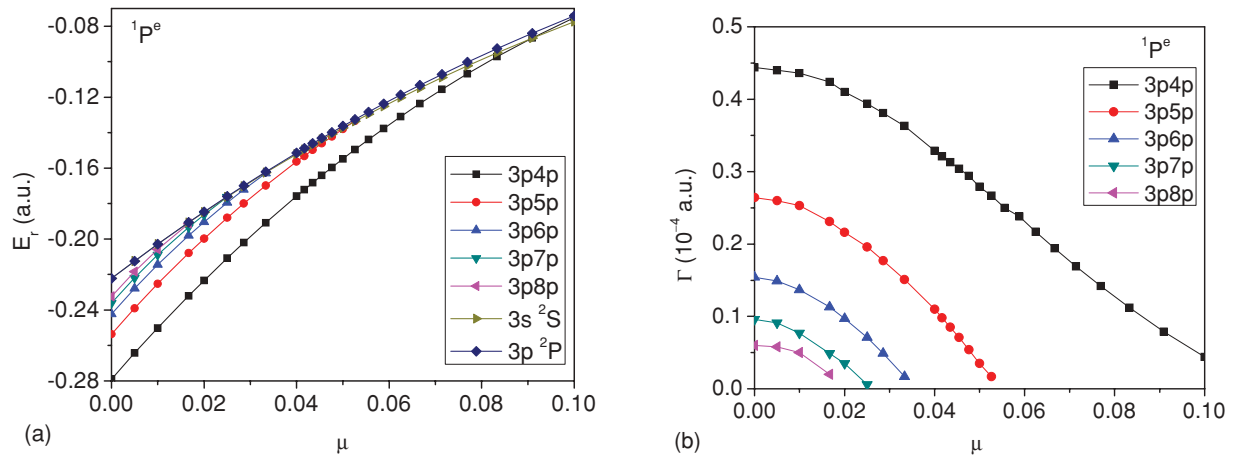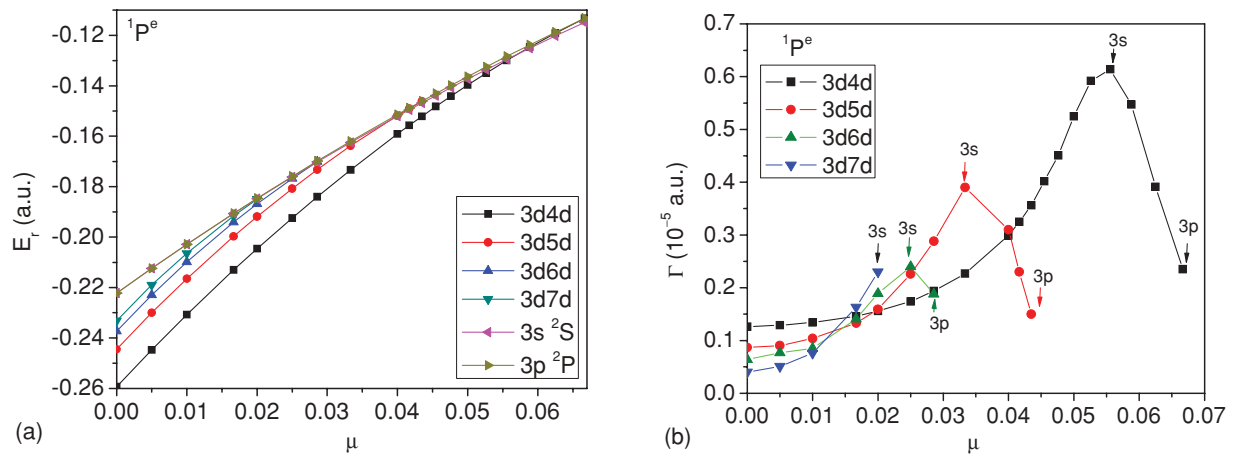$^a$Our previous work with CI-type basis functions [19].

FIG. 3. (Color online) The $3pnp$ $^1P^e$ resonance (a) energies and (b) widths of He in terms of the screening parameter $\mu$ (units of $a_0^{-1}$), along with the He($3s$ $^2S$) and He($3p$ $^2P$) threshold energies.
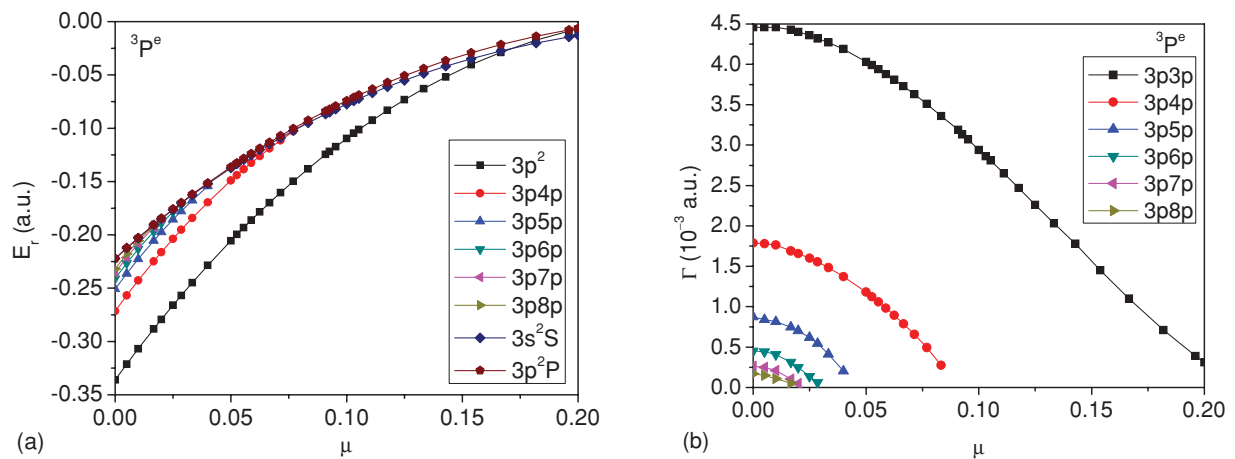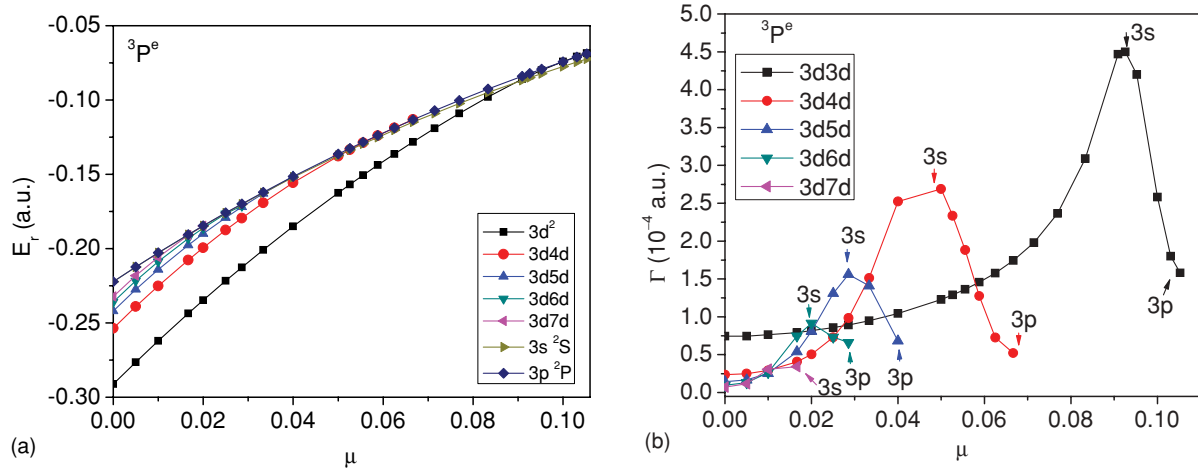


FIG. 4. (Color online) The $3dnd$ $^1P^e$ resonance (a) energies and (b) widths of He in terms of the screening parameter $\mu$ (units of $a_0^{-1}$), along with the He($3s$ $^2S$) and He($3p$ $^2P$) threshold energies.



FIG. 5. (Color online) The $3pnp$ $^3P^e$ resonance (a) energies and (b) widths of He in terms of the screening parameter $\mu$, along with the He($3s$ $^2S$) and He($3p$ $^2P$) threshold energies.

FIG. 6. (Color online) The $3dnd$ $^3P^e$ resonance (a) energies and (b) widths of helium in terms of the screening parameter $\mu$ (units of $a_0^{-1}$), along with the He($3s\,^2S$) and He($3p\,^2P$) threshold energies.

with increasing screening strength and, ultimately, close to the H($3p\,^2P$) threshold. The resonance state lying above the $^2S$ threshold corresponds to the shape resonance, and the one lying below the $^2S$ threshold corresponds to the Feshbach resonance. Between the two series of resonances, the $3pnp$ series shows the decreasing resonance width with increasing screening strength, while the $3dnd$ series shows increasing resonance width up to the $3s\,^2S$ threshold and then starts to decrease up to the $3p\,^2P$ threshold. For the helium atom, we use a maximum of 800-term wave functions for the calculations using the complex-coordinate rotation method, and 600-term wave functions for the stabilization method. We use a maximum of 700-term wave functions for the hydrogen negative ion. Finally, we discuss possible applications of our predicted results in the presence of a plasma background. At present, the theoretical results might be used for plasma diagnostic purposes. Perhaps in the future, investigations of laboratory plasmas will have advanced such that the temperature and charge density of plasma are in controllable conditions, and the Debye length can be adjusted in experiments. When such conditions are achieved in laboratories, experimental measurements of some shifted transitions for plasma-embedded helium impurities can be used, in turn, to test the theoretical predications.

## IV. CONCLUSIONS

In the present work, we have investigated the $^{1,3}P^e$ resonance states of helium and the hydrogen negative ion interacting with screened Coulomb potentials using highly correlated wave functions in the framework of the stabilization method. We have presented two series for resonances below the $N = 3$ threshold, between which $3dnd$ resonance states of He exhibit increasing resonance width for Feshbach resonance states and decreasing behavior for the shape resonance states in between the $3s$ and $3p$ thresholds of He$^+$ for increasing screening strength, and $3pnp$ states exhibit decreasing resonance widths both for the Feshbach and shape resonances. We have also made a comparison between the results using CI-type basis functions and correlated basis functions. The $3p4p$ $^{1,3}P^e$ resonance states of the hydrogen negative ion exhibit similar behavior as the helium atom. In free atomic cases, we have also investigated the $^{1,3}P^e$ resonance states of He using the stabilization method and the complex-coordinate rotation method. Few $^1P^e$ resonance states of helium below the $N = 4$ and 5 thresholds are reported using correlated wave functions. In this work, we have included a brief discussion of the $5p^2$ $^3P^e$ resonance state of the helium atom for the pure Coulomb case in the context of a recent report [21].

[1] S. Kar and Y. K. Ho, Phys. Rev. A **79**, 062508 (2009); **80**, 062511 (2009).

[2] S. Kar and Y.K. Ho, J. Phys. B **42**, 044007 (2009), and references therein.

[3] A. N. Sil, S. Canuto, and P. K. Mukherjee, Adv. Quantum Chem. **58**, 115 (2009).

[4] A. Basu, Euro. Phys. Lett. **88**, 53001 (2009).

[5] V. L. Jacobs, Phys. High Energy Density **5**, 80 (2009).

[6] J. K. Saha, S. Bhattacharyya, T. K. Mukherjee, and P. K. Mukherjee, J. Phys. B **42**, 245701 (2009); M. Pawlak, M. Bylicki, S. Bhattacharyya, T. K. Mukherjee, and P. K. Mukherjee, *ibid.* **42**, 215701 (2009).

[7] F. Pont and P. Serra, Phys. Rev. A **79**, 032508 (2009).

[8] S. B. Zhang, J. G. Wang, and R. K. Janev, Phys. Rev. Lett. **104**, 023203 (2010); Phys. Rev. A **81**, 032707 (2010).

[9] S. Kar and Y. K. Ho, Int. J. Quantum Chem. **110**, 993 (2010), and references therein.

[10] A. Basu, J. Phys. B **43**, 115202 (2010).

[11] S. Kar and Y. K. Ho, Phys. Rev. A **81**, 062506 (2010).

[12] S. B. Zhang, Y. Y. Qi, Y. Z. Qu, X. J. Chen, and J. G. Wang, Chin. Phys. Lett. **27**, 013401 (2010); S. B. Zhang, J. G. Wang, R. K. Janev, Y. Z. Qu, and X. J. Chen, Phys. Rev. A **81**, 065402 (2010).

[13] A. Ghoshal and Y. K. Ho, J. Phys. B **43**, 115007 (2010); S. Paul and Y. K. Ho, Phys. Plasmas **17**, 08704 (2010); C. Y. Lin and Y. K. Ho, *ibid.* **17**, 093302 (2010).

[14] M. C. Zammit, D. V. Fursa, and I. Bray, Phys. Rev. A **82**, 052705 (2010).

[15] J. K. Saha, S. Bhattacharyya, T. K. Mukherjee, and P. K. Mukherjee, J. Quant. Spectrosc. Radiat. Transfer **42**, 111 (2010).

[16] S. Kar and Y. K. Ho, J. Phys. B **43**, 015001 (2010).

[17] S. Chakraborty and Y. K. Ho, Chem. Phys. Lett. **438**, 99 (2007).

[18] S. Kar and Y. K. Ho, Phys. Rev. E **70**, 066411 (2004), and references therein; Chem. Phys. Lett. **402**, 544 (2005); New J. Phys. **7**, 141 (2005); Phys. Rev. A **72**, 010703 (2005); **73**, 032502 (2006); Few-Body Syst. **40** 13 (2006); J. Phys. B **39**, 2445 (2006); Phys. Rev. A **75**, 062509 (2007); Euro. Phys. J. D **48**, 157 (2008); Few-Body Syst. **46**, 173 (2009).

[19] S. Kar and Y. K. Ho, J. Phys. B **40**, 1403 (2007).

[20] S. Kar and Y. K. Ho, Phys. Rev. A **82**, 036501 (2010).

[21] J. K. Saha and T. K. Mukherjee, Phys. Rev. A **82**, 036502 (2010).

[22] L. Lipsky, R. Anamia, and M. J. Colnnely, At. Data Nucl. Data Tables **20**, 127 (1977).

[23] Y. K. Ho and A. K. Bhatia, Phys. Rev. A **47**, 2628 (1993).

[24] L. Argenti and R. Moccia, J. Phys. B **40**, 3655 (2007).

[25] J. K. Saha and T. K. Mukherjee, Phys. Rev. A **80**, 022513 (2009).

[26] J. Eiglsperger, B. Piraux, and J. Madroňero, Phys. Rev. A **81**, 042528 (2010).

[27] Y. K. Ho and J. Callaway, J. Phys. B **17**, L559 (1984), and references therein.

[28] Y. K. Ho and J. Callaway, Phys. Rev. A **27**, 1887 (1983); **34**, 130 (1986).

[29] Y. K. Ho, Phys. Rev. A **50**, 4877 (1994), and references therein.

[30] M. Bylicki and C. A. Nicolaides, J. Phys. B **32** L317 (1999); **33**, 911 (2000).

[31] S. Kar and Y. K. Ho, J. Phys. B **42**, 185005 (2009).

[32] J. L. Tech and J. F. Ward, Phys. Rev. Lett. **27**, 367 (1971), and references therein.

[33] H. G. Berry *et al.*, Phys. Rev. A **3**, 1934 (1971), and references therein; **6**, 600 (1972), and references therein.

[34] V. A. Mandelshtam, T. R. Ravuri, and H. S. Taylor, Phys. Rev. Lett. **70**, 1932 (1993).

[35] J. Müller, X. Yang, and J. Burgdörfer, Phys. Rev. A **49** 2470 (1994).

[36] S. S. Tan and Y. K. Ho, Chin. J. Phys. **35**, 701 (1997).

[37] S. Kar and Y. K. Ho, J. Phys. B **37**, 3177 (2004).

[38] Y. K. Ho, Phys. Rep. **99**, 1 (1983).

[39] A. M. Frolov and V. H. Smith Jr., Phys. Rev. A **53**, 3853 (1996).

[40] S. Kar and Y. K. Ho, J. Phys. B **42**, 055001 (2009); **43**, 135003 (2010).

[41] E. Braendas and P. Froehlich, Phys. Rev. A **10**, 1612 (1977).

[42] N. Moiseyev, P. R. Certain, and F. Weinhold, Mol. Phys. **36**, 1613 (1978).

[43] R. Yaris and P. Winkler, J. Phys. B **11**, 1475 (1978).

[44] P. Winkler and R. Yaris, J. Phys. B **11**, 1481 (1978).

[45] P. Winkler and R. Yaris, J. Phys. B **11**, 4257 (1978).

[46] L.S. Cederbaum and P. Winkler, Theor. Chim. Acta **88**, 257 (1994).